

Advanced cavity detection in ground penetrating radar B-scan image using fully convolutional networks

Sayali Pangavhane¹, Dinh-Viet Le² and Gyu-Hyun Go^{*1}

¹School of Architecture, Civil and Environmental Engineering, Kumoh National Institute of Technology, 61, Daehak-ro, Gumi-si, Gyeongsangbuk-do, Republic of Korea

²Ground Reinforcement Technology Research Institute, Kumoh National Institute of Technology, 61, Daehak-ro, Gumi-si, Gyeongsangbuk-do, Republic of Korea

(Received November 19, 2024, Revised March 6, 2025, Accepted March 25, 2025)

Abstract. Detecting underground cavities and voids is critical for ensuring structural safety in sectors such as civil engineering and environmental studies. Ground Penetrating Radar (GPR) B-scan imaging is a valuable tool for this purpose, yet traditional methods often struggle with precise cavity characterization, especially as cavities develop over time. Addressing this gap, this study introduces an advanced methodology using Fully Convolutional Networks (FCNs) to improve cavity detection accuracy across four progressive stages: Initial, Intermediate, Critical, and Damaged. The GUI based KIT-GPR model, trained on Finite Difference Time Domain (FDTD) simulated data, can identify cavities as they grow from small initial voids to significant structural threats. This method influences GUI programming, enabling non-experts to interpret B-scan images more intuitively. Key findings indicate that while the KIT-GPR model demonstrates potential in cavity detection across different developmental stages, it faces challenges in accurately identifying and classifying cavities, particularly in complex scenarios. These limitations highlight the need for further refinement to improve detection reliability in GPR analysis and enhance its applicability in subsurface imaging and infrastructure monitoring.

Keywords: B-scan; cavity detection; Finite Difference Time Domain (FDTD); Fully Convolutional Networks (FCNs); Ground Penetrating Radar (GPR); GUI programming

1. Introduction

Road structures are designed to support vehicular traffic and provide safe, efficient, and durable transportation. These structures typically consist of several layers, each serving a specific function to ensure road stability, strength, and longevity. They are engineered to handle various stresses caused by traffic and environmental conditions (Wang *et al.* 2024). A good design, choice of materials, and maintenance will ensure that the road performs well and is safe over a long period. Stabilization techniques, such as using agricultural waste additives, have been explored to enhance the stability of expansive soils, contributing to stronger subsurface foundations (Gidebo *et al.* 2023). However, the visible pavement is not the sole factor in road strength, with much of its durability depending on the quality and integrity of the underlying layers. Therefore, focusing on these foundational layers is essential, as they provide support for the entire road (Sato and Kuwano 2025). Sinkholes and cavities weaken these foundations, making roads more susceptible to damage, cracks, and eventual collapse, which poses risks to drivers and pedestrians (Liu *et al.* 2024). Studies have shown that subsurface anomalies, such as voids and cavities, can disrupt load distribution and compromise foundation

stability (Basha and Eldisouky 2023). Non-invasive techniques like ground-penetrating radar (GPR) and electromagnetic surveys have become crucial for early detection, enabling proactive maintenance and reducing road safety risks before surface damage occurs (Shi 2022). By identifying these weaknesses in advance, engineers can prevent accidents (Fig. 1), minimize traffic disruptions, and extend the lifespan of road structures. Recent advancements in Artificial Intelligence (AI) based GPR analysis, particularly deep learning techniques like Transformers and attention mechanisms, have further enhanced defect detection. For instance, Zhang *et al.* (2019) and Dawood *et al.* (2020) highlighted how advanced GPR techniques, such as Full Waveform Inversion (FWI) and Reverse Time Migration (RTM), improve defect detection accuracy in subsurface imaging. Additionally, Huang *et al.* (2024) introduced a self-supervised framework for GPR data, further enhancing flaw detection and analysis. As deep learning techniques evolve, methods such as Transformers and attention mechanisms are increasingly applied in GPR analysis, drawing from their success in natural language processing and image recognition to enhance pattern identification in large datasets. In our study, we contribute to these advancements by utilizing a Fully Convolutional Network (FCN) in the development of KIT-GPR for simulation, establishing a foundation for integrating more sophisticated techniques like attention mechanisms in future research.

*Corresponding author, Professor
E-mail: gyuhungo@kumoh.ac.kr



Fig. 1 Example of sinkhole formation in road structures leading to vehicle accidents (Source: Yonhap News)

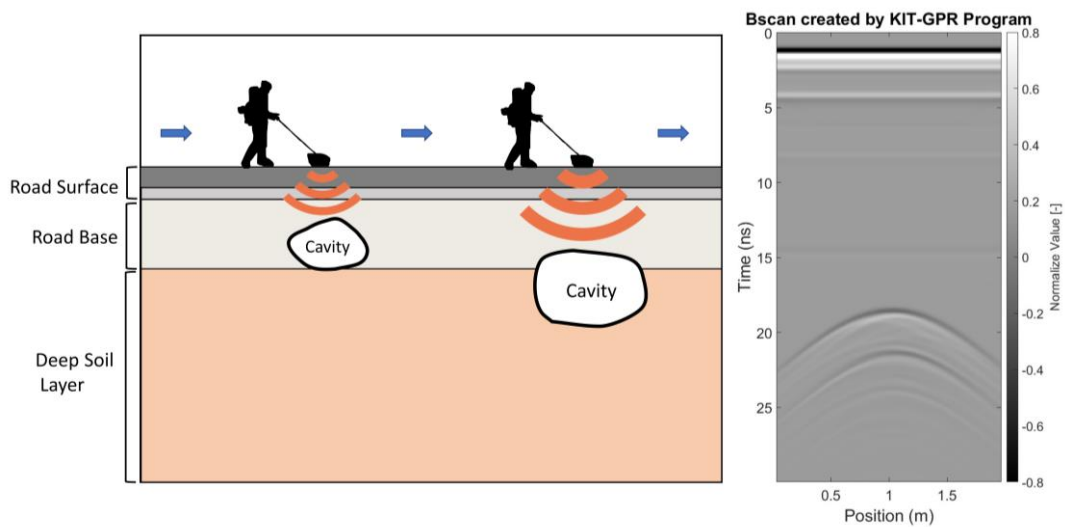


Fig. 2 Schematic representation of GPR scanning the subsurface cavities and corresponding B-scan

GPR is a non-destructive, high-resolution geophysical method that utilizes high-frequency electromagnetic waves for subsurface structural imaging (Min and Yoon 2024). It transmits radar pulses into the ground and records the signals reflected back from various underground materials (Fig. 2). This reflection provides data that can be analyzed to detect and map underground cavities, objects, and structures. GPR is widely used across several industries, including civil engineering, archaeology, geology, and environmental studies (Lai *et al.* 2017). It is particularly valuable for identifying hidden subsurface anomalies such as voids, cavities, and sinkholes beneath roads that are barely visible to the naked eye (Zhang *et al.* 2023).

Detecting cavities in road structures is essential for ensuring road safety and longevity. By identifying subsurface anomalies, engineers can proactively address potential hazards before they evolve into severe issues like sinkholes (Yamaguchi *et al.* 2022). Early detection enables timely maintenance and repair, which minimizes costly damages and reduces risks to public safety (Jena *et al.* 2024). Additionally, modern methods like GPR provide non-destructive, high-resolution imaging, allowing for effective cavity detection without causing surface damage to the road, which further

preserves the road infrastructure (Kang *et al.* 2022). Although cavity detection provides numerous benefits, it also has certain limitations. The technology and equipment required, such as GPR, can be costly to purchase and operate, making it less accessible for smaller municipalities or underfunded departments. Detection accuracy can be affected by factors such as soil type, moisture levels, and road material composition, potentially resulting in false positives or missed cavities. Furthermore, interpreting the data from GPR scans or other imaging tools requires skilled personnel and advanced software, which can add to operational costs.

B-scan imaging is one of the most widely used techniques for visualizing GPR data, offering a cross-sectional view of the subsurface to help experts assess cavity depth, size, and location (Kim *et al.* 2024). During scanning, the GPR system emits electromagnetic pulses that reflect off subsurface structures, generating a detailed visualization of underground conditions. This enables precise identification of cavity formation (Balasubramani and Gopalakrishnan 2020). The ability of B-scan imaging to provide crucial insights makes it a valuable tool for making informed repair decisions and implementing preventive measures. By carefully analyzing these scans, engineers can

accurately pinpoint problem areas (Guerrieri *et al.* 2024). Despite its effectiveness, interpreting B-scans can be challenging due to the complexity of radar signal reflections (Fig. 2). Variations in subsurface materials, moisture content, and cavity shapes often create intricate patterns that require expert analysis (Min *et al.* 2018). This interpretation process is typically time-intensive and susceptible to human error. To overcome these limitations, automated cavity detection models have been developed to process B-scan data more efficiently. By leveraging advanced algorithms and machine learning techniques, these models enhance detection accuracy while reducing the need for expert intervention (Tong *et al.* 2020).

In this study, we introduce KIT-GPR, a graphical user interface (GUI)-based GPR program designed to improve both accuracy and usability in cavity detection. This model utilizes a Fully Convolutional Network (FCN) powered by deep learning to automatically identify and classify cavities in B-scan images with minimal human effort. By training on extensive datasets, KIT-GPR learns distinctive patterns and features associated with subsurface cavities (Abdelmawla *et al.* 2023). Once trained, it can analyze new GPR scans, providing accurate visual representations of cavity locations, sizes, and depths. By simplifying the traditionally complex process of B-scan interpretation, KIT-GPR serves as an efficient and reliable tool for road maintenance professionals. The deep learning model predicts underground structures from B-scan images in two key stages. First, it extracts essential features using multiple convolutional layers while reducing image size through pooling layers, enabling the model to focus on key patterns. In the second stage, the model reconstructs the image into a predicted underground geometry using deconvolution layers to restore the original dimensions. Additionally, connections between layers help retain critical details for improved accuracy. This approach effectively detects hidden structures or defects beneath the surface, making it a powerful tool for subsurface analysis.

2. Methodology

This study proposes a three-stage framework for detecting and evaluating cavities beneath road infrastructures using Ground Penetrating Radar (GPR) simulations. The core of this framework relies on **KIT-GPR**, a custom GPR simulation software, and an image analysis model based on Fully Convolutional Networks (FCNs). This GUI-based GPR tool utilized the finite difference time domain (FDTD) method to simulate electromagnetic wave propagation, enabling detailed subsurface imaging and cavity detection. Additionally, the FCN model performs dense pixel-wise predictions, facilitating automated analysis of subsurface anomalies in the generated GPR images. This section outlines the methodology in detail, covering both the simulation and image analysis techniques.

2.1 FCNs

The image analysis portion of this study utilizes FCNs, a type of neural network specifically designed for dense

prediction tasks. FCNs are ideal for semantic segmentation tasks, as they allow pixel-wise classification of image data without requiring fixed-size inputs. Unlike traditional convolutional neural networks (CNNs) (which rely on fully connected layers that restrict input and output sizes), FCNs replace these layers with convolutional layers, making them highly adaptable for variable-sized input data, as often required in GPR image analysis. Previous studies have demonstrated the effectiveness of CNNs in detecting subsurface anomalies in GPR data, underscoring the potential of neural networks for cavity detection in roadway infrastructure (Shrestha and Zhihou 2024). Building on these insights, our study employs FCNs to improve adaptability and precision in anomaly classification.

The structure of an FCN enables high-resolution output predictions through upsampling operations, which restore the spatial resolution of the feature maps to match the original image size. This upsampling process is critical for generating precise, pixel-level predictions in the B-scan images, which depict subsurface layers and cavities. Furthermore, the inclusion of **skip connections** in the network architecture allows for the integration of lower-layer spatial details with higher-layer semantic information, enhancing accuracy by preserving fine structural details in the output. During training, the FCN model evaluates the difference between the predicted and actual pixel labels using a cross-entropy loss function:

$$L = - \sum_i y_i \log(\hat{y}_i) \quad (1)$$

where y_i denotes the ground truth label for pixel i , with \hat{y}_i being the predicted probability for that pixel. This loss function is optimized to ensure accurate boundary detection and segmentation of cavities, allowing the model to effectively distinguish between different cavity stages.

2.2 FDTD method

The KIT-GPR simulation software implements the Finite Difference Time Domain (FDTD) method, a numerical approach for solving Maxwell's equations and modeling electromagnetic wave propagation in GPR simulations. This method is well-suited for detecting subsurface material variations, as it accurately simulates the interaction of electromagnetic waves with different media. Compared to other numerical techniques, such as ray-based, frequency-domain, integral, and pseudo-spectral methods, FDTD is widely used due to its ability to incorporate key physical parameters, including conductivity (σ), dielectric constant (ϵ), and magnetic permeability (μ). Its effectiveness in GPR simulations has been demonstrated through established tools such as MATLAB-based FDTD models (Irving *et al.* 2006) and gprMax (Warren *et al.*, 2016), further validating its applicability in subsurface imaging and cavity detection. Maxwell's equations, which describe the behavior of electric (E) and magnetic (H) fields, serve as the basis of the FDTD approach

$$\nabla \times E = - \frac{\partial B}{\partial t} \quad (2)$$

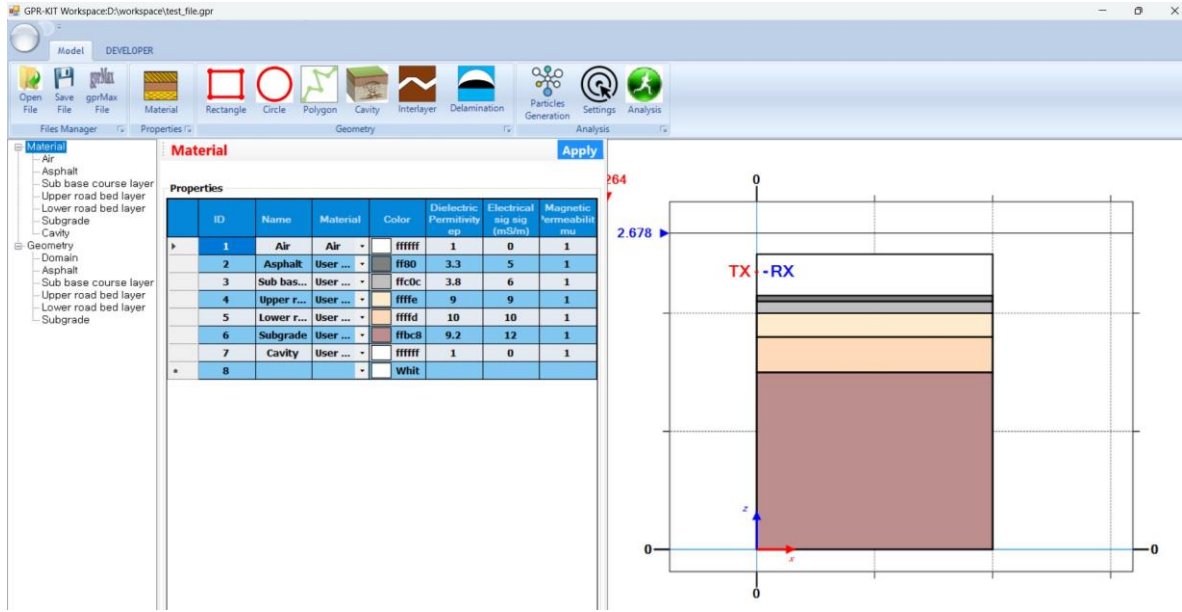


Fig. 3 Arrangement of material parameters and Domain setup in GUI based GPR interface

$$\nabla \times H = J + \frac{\partial D}{\partial t} \quad (3)$$

where D is the electric displacement field, J represents the current density, and B denotes the magnetic flux density. These equations are discretized in both time and space, allowing for a time-stepped solution across a computational grid. The resulting time-update equations for the electric and magnetic fields facilitate the simulation of wave propagation through different materials at each time step.

2.3 GUI based GPR program (KIT-GPR)

The GUI-based GPR program, KIT-GPR, is a specialized simulation tool developed in C# that uses the FDTD method widely applied in GPR analysis for simulating electromagnetic wave propagation in various media. KIT-GPR includes several essential modules (Fig. 3) such as the Material Declaration Module, Geometry Construction Module, Antenna Parameter Declaration Module, and Analysis Module. These modules allow users to configure, simulate, and analyze the subsurface structures under investigation.

In the **Material Declaration Module**, users can define key properties of various materials found in subsurface structures, such as the dielectric constant (ϵ), electrical conductivity (σ), and magnetic permeability (μ). These material properties significantly affect wave propagation, reflection, and attenuation, playing a crucial role in accurately simulating the subsurface environment. Users can select from pre-defined materials or input custom material parameters based on the specific characteristics of the infrastructure under study. The **Geometry Construction Module** enables users to create customized subsurface models by defining the geometry of different regions, including rectangular, circular, or polygonal areas, and assigning corresponding material properties to these

regions. By assigning color codes to each material type, this module allows for easy visual distinction between layers, which is essential when interpreting GPR results. The **Antenna Parameter Declaration Module** provides flexibility in configuring the simulation's electromagnetic parameters, such as waveform type, time step, scanning step, and scanning line length. These settings are critical for controlling the resolution and depth of the GPR data, with the software offering a range of pre-configured antenna types sourced from the open-source library **gprMax**. The KIT-GPR program also includes real-time error checking to ensure accuracy and avoid configuration mistakes that could compromise simulation fidelity. Once the setup is complete, the **Analysis Module** facilitates the visualization of simulated GPR data. It dynamically displays A-scan results at each scan position and generates B-scan images, offering a two-dimensional cross-sectional view of the subsurface. This real-time visualization enables users to observe wave patterns and identify potential anomalies, such as voids or cavities.

2.4 Model simulation

In the KIT-GPR program, the material parameters shown in Table 1 are used for defining the geometry in GPR simulations, with the geometry layers based on Korea's road design standard (MLIT, 2012). The model comprises distinct layers such as "Air," "Asphalt," "Sub base course layer," "Upper road bed layer," "Lower road bed layer," "Subgrade," and "Cavity," each with assigned specific physical properties dielectric permittivity (ϵ), electrical conductivity (σ), and magnetic permeability (μ). The material parameters data used in this work were collected from various research studies (Li *et al.* 2024). As illustrated in Fig. 3, colors are assigned to each material layer for clear vis differentiation within the software.

Table 1 The material parameters of KIT-GPR

No	Material	Dielectric permittivity ϵ (F/m)	Electrical Conductivity σ (mS/m)	Magnetic permeability μ (H/m)
1	Air	1	0	1
2	Asphalt	3.3	5	1
3	Sub base course layer	3.8	6	1
4	Upper road bed layer	9	9	1
5	Lower road bed layer	10	10	1
6	Subgrade	9.2	12	1
7	Cavity	1	0	1

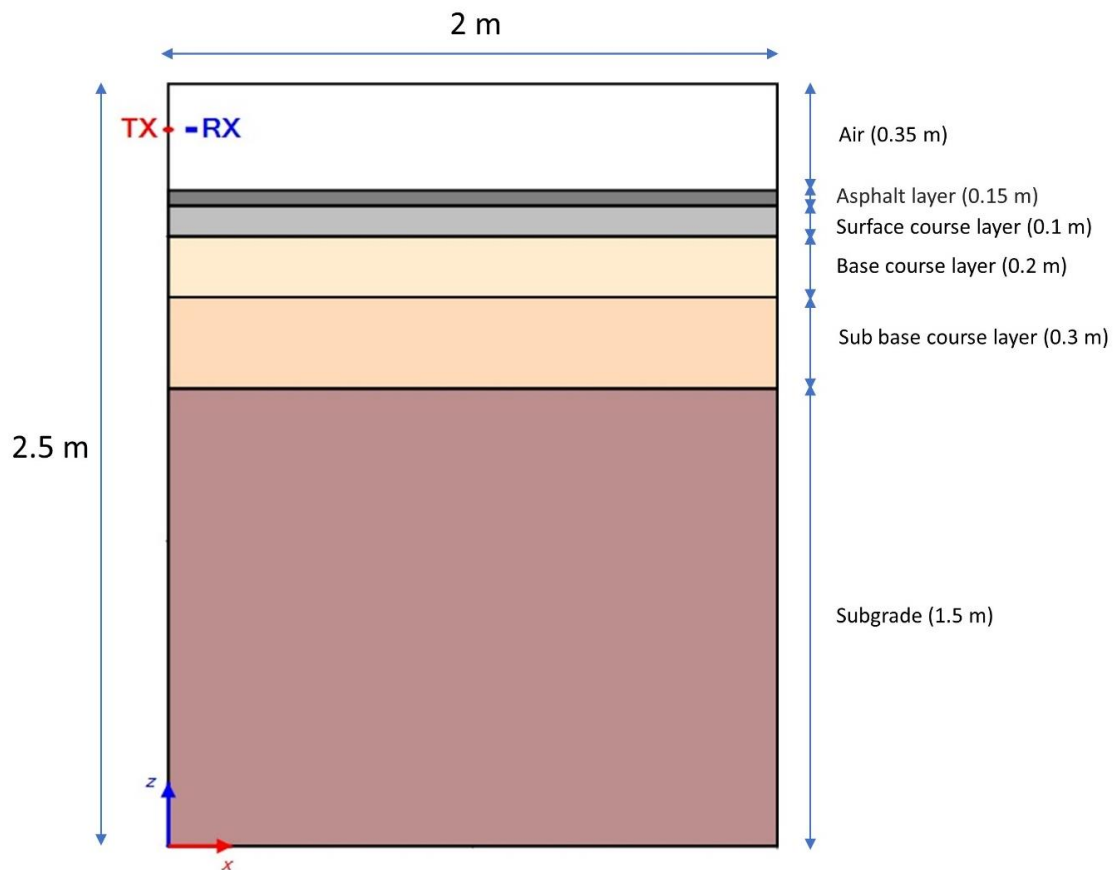


Fig. 4 Domain configuration of pavement layers with dimensions for KIT-GPR simulation

After setting up the material parameters in the KIT-GPR program, the domain for the cross-sectional visualization of the road was created. The KIT-GPR model domain (Fig. 4) represents a 2-m-wide by 2.5-m-deep cross-sectional view of a layered road structure for GPR analysis. This model illustrates a typical road section and its subgrade layers, crucial for understanding subsurface conditions. At the top, a 0.35-m air layer represents free space essential for radar wave transmission. Followed by a 0.15-m asphalt layer simulating the road surface and a 0.1-m surface course layer that enhances durability and load distribution. Beneath this, a 0.2-m base course provides structural support and improves drainage, while a 0.3-m sub-base course offers frost protection and additional load distribution. The deepest layer, the 1.5-m subgrade, forms the foundational

soil beneath the road, playing a critical role in road stability. Variations in the subgrade, such as voids or density changes, are key focus areas for GPR analysis. In the top-left corner, the labels “TX” and “RX” indicate the positions of the GPR transmitting and receiving antennas, which emit and detect radar waves as they pass through each layer. These waves reflect differently depending on the material properties and thickness of each layer, enabling the identification of subsurface anomalies. The inset on the right provides further details on layer composition, showing specific materials and thicknesses commonly used in pavement construction, such as coarse aggregate or specific asphalt types. These material details are integral for defining the dielectric properties in the KIT-GPR simulation, which then predicts wave behavior and helps

Table 2 The model and antenna setting parameters of KIT-GPR

No	Name of the parameter	Value
1	Domain (m)	2.5m x 2m
2	dx, dy, dz (m)	0.005, 0.005, 0.0069
3	Time window (s)	3×10^{-8}
4	Antenna type	MALA 1.2 GHz
5	Waveform type	Gaussian
6	Scanning step (m)	0.01
7	Number of Perfectly Matched Layer (PML) boundaries	20 cell

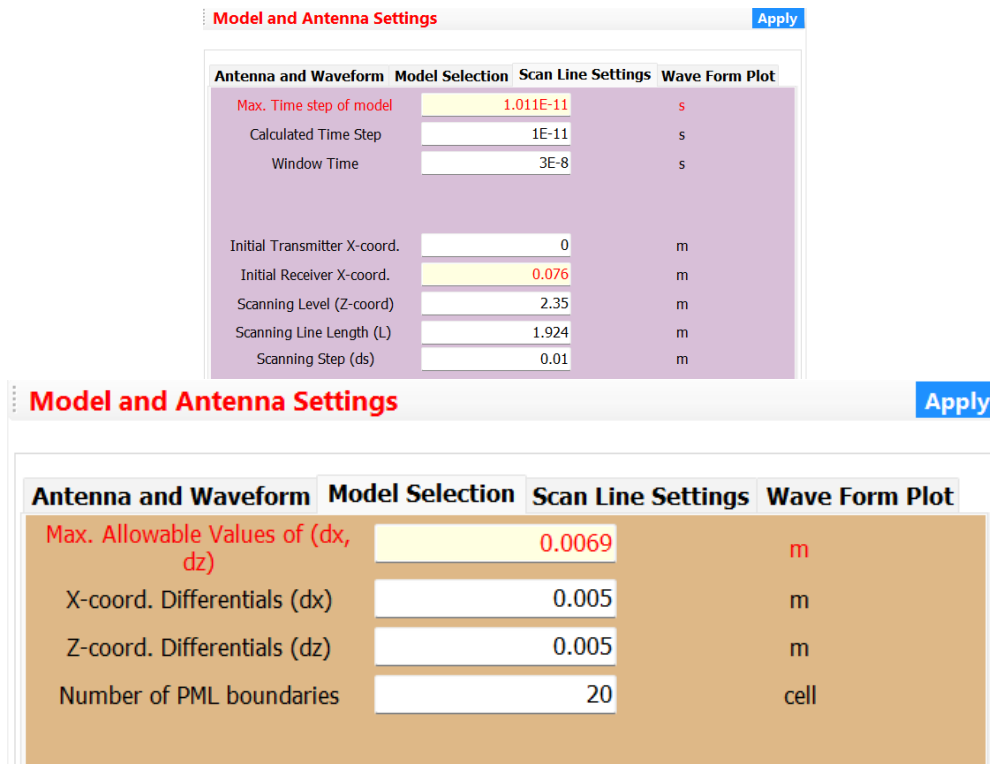


Fig. 5 Model and Antenna setting in KIT-GPR program

identify potential road integrity issues like voids, cracks, or density anomalies within the subsurface structure.

To capture accurate subsurface data, the KIT-GPR model incorporates specific scanning and antenna parameters (Table 2), including scanning resolution, time window, and waveform characteristics. The GPR system, represented in the top-left corner as "TX" and "RX," consists of transmitting and receiving antennas that emit and detect radar waves as they pass through each layer. These waves reflect differently based on material properties, enabling anomaly detection. Fig. 5 details the model's antenna configuration, highlighting key specifications such as antenna type (MALA 1.2 GHz), source resistance, baseline length, and waveform type (Gaussian), which influence signal characteristics. Additionally, waveform amplitude, excitation frequency, and maximum frequency are set to optimize depth penetration and resolution. Scan line configurations, including scanning level, length, and step size, ensure

precise spatial resolution, enhancing subsurface imaging accuracy.

The capabilities of KIT-GPR in simulating subsurface conditions have been further explored in our conference presentation at the KGS Spring National Conference 2024 (Le and Go 2024). This work provides additional insights into the application of KIT-GPR for ballast railway ground assessment, demonstrating its effectiveness in identifying fouled layers through simulation. While the modeled B-scans in this study were not directly validated with real experiments, the findings presented in the conference further support the accuracy and applicability of the proposed approach.

In numerical GPR modeling, the domain is structured as a grid of points, encompassing both the interior region and a boundary layer known as the Perfectly Matched Layer (PML) (Gedney 2011). PML is a specialized material layer, that absorbs outgoing waves to prevent reflections from returning into the model's interior, simulating an infinite

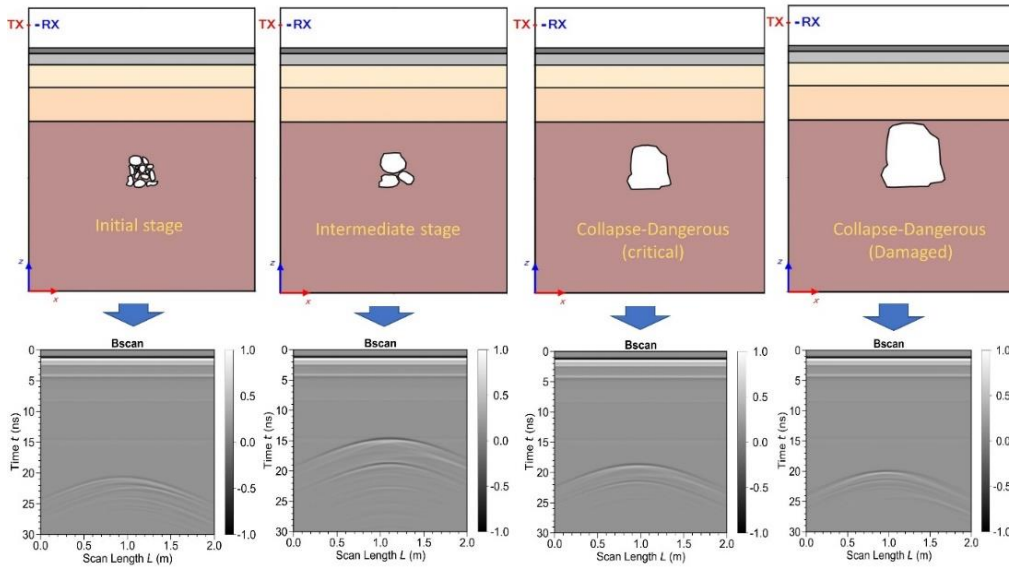


Fig. 6 Comparison of stages of cavity development in subgrade layer and corresponding GPR B-scan

space within a finite domain. The interior grid points correspond to user-defined material properties, while the boundary points are assigned PML material properties designed for wave absorption (Irving and Knight 2006). Although default PML settings are often used, they can be customized to enhance simulation accuracy. By integrating these material, model, and antenna parameters, the KIT-GPR simulation ensures optimized subsurface detection, facilitating the identification of road integrity issues such as voids, cracks, or density anomalies within pavement layers.

2.5 Dataset creation and B-scan

This paper introduces a four-stage framework for detecting deep cavities in subsurface infrastructures. The dataset is based on four different cavity growth scenarios (Fig. 6), which were manually created using WebPlotDigitizer. This computer vision-assisted software helps extract numerical data from images of various data visualizations (WebPlotDigitizer, <https://automeris.io/WebPlotDigitizer/>). The generated CSV files from WebPlotDigitizer were then input into the KIT-GPR program to simulate these scenarios. In total, 200 dataset cases were created, divided into four cavity stages, Initial stage, Intermediate stage, Collapse-Dangerous stage (Critical), and Collapse-Dangerous stage (Damaged). For each stage, 50 different cases were generated, each featuring the same overall geometry but varying in cavity shape and size to reflect realistic underground conditions. In the Initial stage, the cavities are small and newly formed beneath the road structure. At this point, the cavities consist of several small, fragmented voids that pose minimal risk to road stability. The KIT-GPR program is used to simulate this geometry, and MATLAB generates the B-scan image that corresponds to this scenario. The B-scan image shows a slight, curved anomaly at the subsurface level, indicating the presence of small cavities. These variations allow the program to train effectively for early-stage cavity detection.

In the Intermediate stage, the cavities begin to expand in size. While they have not yet reached critical dimensions, these enlarging cavities pose an increasing risk to the road's structural integrity. The B-scan image produced by MATLAB during this stage reveals a more pronounced anomaly compared to the Initial stage. The curve seen in the B-scan is larger, indicating the growing presence of the cavity beneath the surface. The Collapse-Dangerous stage combines two stages. In the Collapse-Dangerous (Critical) stage, the cavities have expanded considerably, nearing a size where they could start causing subsurface damage. At this stage, the cavity is large enough to potentially lead to the formation of sinkholes or other subsurface issues if left untreated. The B-scan image generated during this stage clearly shows a much more pronounced and broader curvature, indicative of the larger cavity below the surface.

In the final Collapse-Dangerous (Damaged) stage, the cavities have reached a point, posing an imminent risk to the road structure. These large cavities represent a severe threat, potentially causing the collapse of the road surface. In the model simulation and evaluation of the results, the B-scan plays an important role in visualizing the data and extracting information from geological cross-sections. The B-scan is formed by compiling A-scan data, each representing a measurement at a specific output data location in the KIT-GPR program. The output data location is used in the MATLAB program to generate the B-scan.

3. Results and discussion

This study successfully demonstrates a framework to detect and evaluate cavity growth beneath road infrastructure using the KIT-GPR program and FCNs for image analysis. The integration of GPR simulation and deep learning methods allows for precise identification and classification of subsurface anomalies, specifically focusing on cavity stages that pose a potential risk to road stability. The process, as

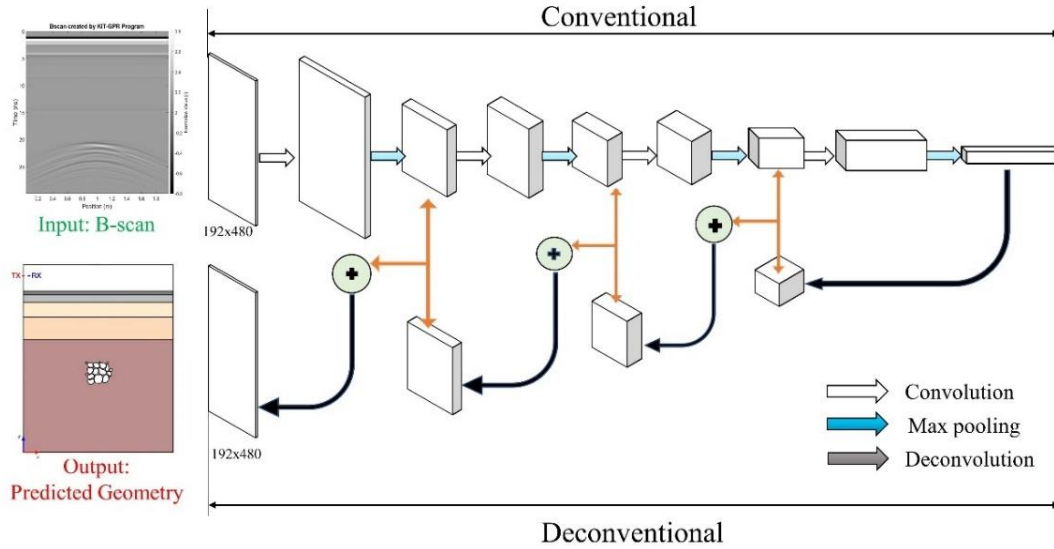


Fig. 7 KIT-GPR Convolutional and Deconvolutional Network for B-Scan to Predicted Geometry

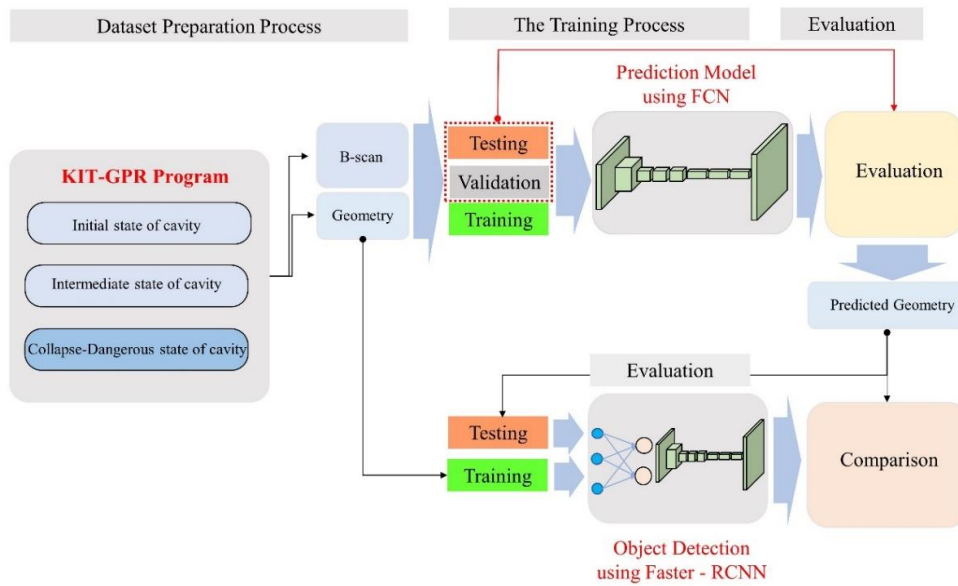


Fig. 8 Schematic of the ANN training process and end user GUI program

shown in Fig. 7, begins with B-scan inputs generated by KIT-GPR, which serve as the foundation for predicting the geometry of subsurface anomalies. The input B-scan, which captures time-domain data across subsurface layers, is processed through an FCN model to produce a spatially accurate predicted geometry output. This process is crucial in identifying cavities with high precision, as seen through the model's capacity to maintain structural details in varying cavity development stages.

Fig. 8 illustrates the dataset preparation, training, and evaluation pipeline for predicting subsurface cavities using the KIT-GPR framework. The dataset includes 200

geometry cases, with 50 cases for each stage of cavity development: Initial, Intermediate, Dangerous-Collapse (Critical), and Dangerous-Collapse (Damaged). Before training, the dataset was shuffled 10 times and split into training, validation, and testing sets to ensure balanced learning. The input consists of B-scan images and corresponding geometries, which are processed by two deep learning models: a Fully Convolutional Network (FCN) for pixel-level segmentation and a Faster Region-Based Convolutional Neural Network (Faster-RCNN) for object detection. The FCN predicts subsurface geometry, while Faster-RCNN identifies the severity of cavity-related risks.

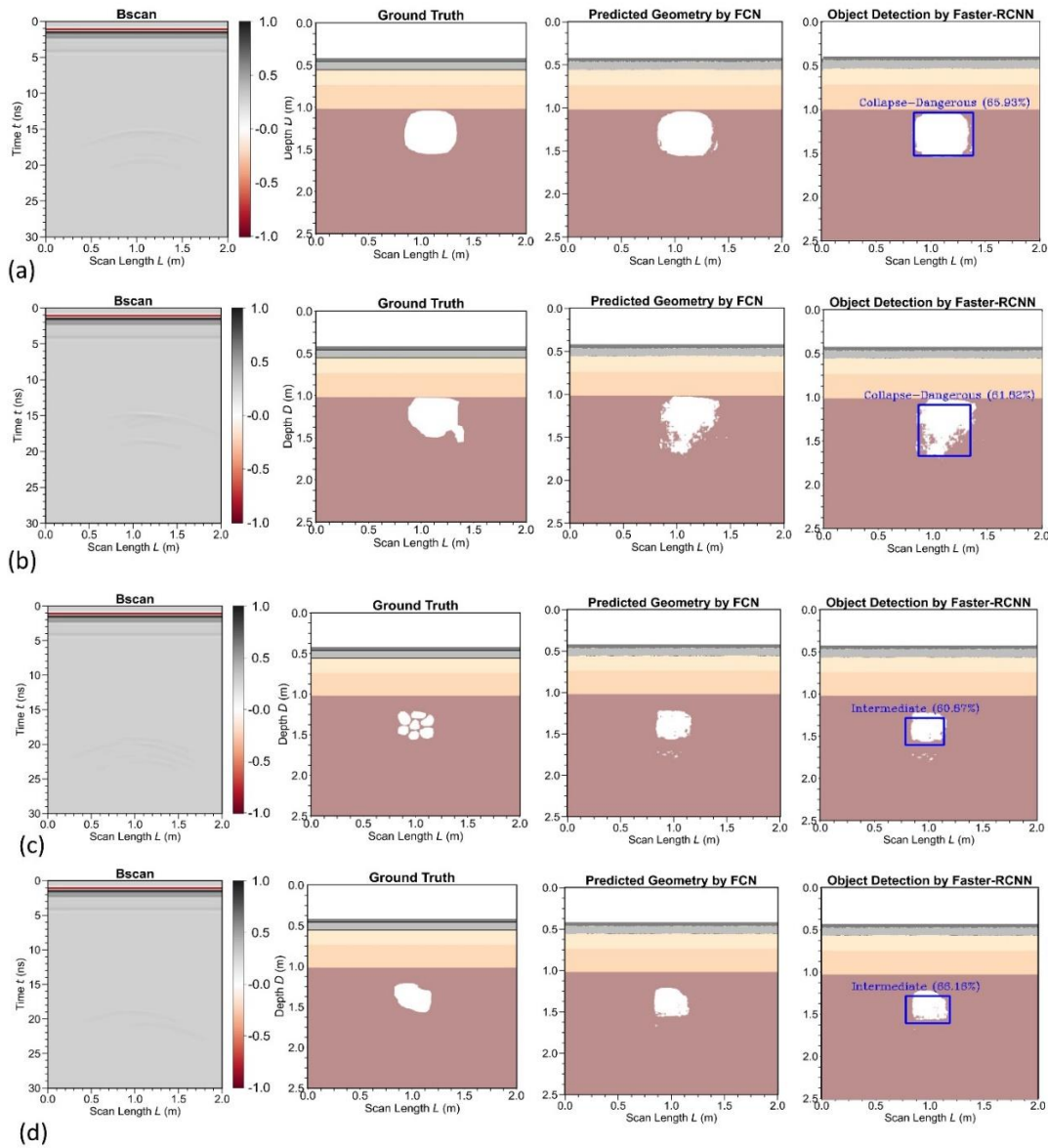


Fig. 9 Comparison of B-scan, Ground truth, predicted geometry, and Object detection by Faster-RCNN

The evaluation phase compares the predicted geometry with actual data to assess the model's accuracy. This process demonstrates the effectiveness of integrating FCNs for geometry prediction and Faster-RCNN for object detection in identifying and classifying cavity structures beneath road infrastructure. Fig. 9 presents four cases of cavity detection, highlighting the model's performance across varying cavity sizes and configurations that represent different stages of cavity development.

In Case (a), the framework successfully detects a well-defined cavity and categorizes it as "Collapse - Dangerous." The FCN accurately captures the geometry of the cavity, closely matching the ground truth. The Faster-RCNN model detects this cavity with a confidence score of 65.93%, reflecting strong reliability in identifying it as a significant structural threat. This case demonstrates the model's effectiveness in detecting well-formed cavities with clear structural features.

Case (b) presents a more irregular cavity shape, introducing a slight noise in the FCN prediction around the edges. Despite this, the Faster-RCNN model successfully categorizes the cavity as "Collapse-Dangerous" with a confidence score of 61.82%. The decreased score reflects the increased complexity of the cavity's irregular shape, yet the model still effectively identifies its high-risk status. This case highlights how cavity irregularities can slightly impact detection accuracy but still allow for successful classification.

In Case (c), the model struggles with cavity detection and classification, leading to a failed detection. This case represents the initial stage of cavity development, where multiple small cavities are clustered together. The early-stage formation challenges the model's ability to distinguish individual cavities within the cluster. The FCN captures the clustered arrangement with some boundary blending, while the Faster-RCNN model detects only one cavity within the

cluster and labels it as “Intermediate” with a confidence score of 60.87%. The lower score reflects the difficulty of detecting cavities in early development stages, where anomalies may not be fully formed or distinct, ultimately resulting in a failed detection of the entire structure.

Case (d) presents a solitary cavity in an intermediate stage with distinct edges. Although the FCN prediction aligns with the ground truth in terms of geometry, the Faster-RCNN model categorizes this cavity as “Intermediate” with a confidence score of 66.18%, indicating moderate certainty. However, the model fails to recognize the full structural complexity of the cavities, which contributes to this case being classified as a failed detection. The lack of precision makes it difficult for the Faster-RCNN to accurately assess the danger stage, leading to misclassifications. These errors highlight the model’s limitations in handling more advanced and irregular cavity formations. One notable challenge encountered during the study was the use of manually-generated anomalies in the dataset. While this approach allowed for a controlled representation of various cavity stages, it also introduced additional noise in certain cases. The manual creation process sometimes led to irregular shapes and boundary variations, which could deviate from natural cavity formations and complicate the model’s ability to accurately identify the anomaly stage. This added noise occasionally affected the FCN’s precision in boundary delineation and the Faster-RCNN’s occasionally affected the FCN’s precision in boundary delineation and the Faster-RCNN’s classification, especially in cases where anomaly shapes were less distinct or fragmented.

The challenges observed in Cases (c) and (d) suggest a need for further refinement in model architecture or training data. Specifically, the FCN’s segmentation performance could benefit from additional tuning or regularization techniques to improve boundary accuracy. Furthermore, expanding the training dataset to include a broader variety of cavity shapes and sizes may help the model generalize better to complex anomalies. These improvements could enhance the model’s ability to accurately predict the stage and severity of cavities in real-world subsurface structures. The integration of FCN and Faster-RCNN in the KIT-GPR framework demonstrates a promising approach to automated subsurface imaging. The FCN model, with its high-resolution segmentation, and the Faster-RCNN model, with its ability to detect and classify dangerous cavities, offer a robust solution for early anomaly detection. This combination enables infrastructure engineers to identify, classify, and prioritize maintenance tasks for subsurface cavities before they escalate into critical structural issues. The high classification confidence scores associated with each stage underscore the model’s potential in real-time monitoring applications, offering substantial advancements over traditional GPR analysis.

4. Conclusions

This research shows a comprehensive framework to enhance subsurface anomaly detection and classification within road infrastructure using GPR simulations. The KIT-

GPR program was utilized for dataset generation, integrating Fully Convolutional Networks for precise pixel-wise segmentation and Faster-RCNN for automated classification of anomaly severity. The main conclusions obtained from the study are as follows:

- The KIT-GPR framework demonstrated effectiveness in detecting early-stage cavities, with the FCN reliably replicating ground truth geometries for various cavity stages. This capability underscores the potential of FCN for precise anomaly mapping, essential for early intervention and maintenance planning in road infrastructure.
- Integrating Faster-RCNN into the framework provided an automated classification layer, enabling accurate identification of both initial and intermediate cavity stages. This advancement contributes to proactive risk assessment by categorizing cavities based on severity, which is crucial for prioritizing maintenance tasks.
- Challenges emerged with manually created anomalies, which introduced noise and irregularities, sometimes impacting prediction accuracy. Additionally, the model encountered limitations with complex cavity shapes in advanced stages, particularly in Cases (c) and (d), where both FCN segmentation and Faster-RCNN classification faced accuracy challenges. These findings highlight the need for refining dataset quality and model parameters to improve robustness against complex, late-stage anomalies.
- Future work focuses on enhancing model performance by incorporating more diverse training samples, particularly those capturing the progressive expansion of cavities and the deformation of surrounding soil. Studying these dynamic changes could improve the model’s ability to predict cavity evolution at different stages, enabling early intervention before significant structural damage occurs. Additionally, fine-tuning model parameters could bolster detection accuracy, paving the way for a real-time GPR-based anomaly monitoring system. This advancement has the potential to revolutionize infrastructure assessment, leading to proactive maintenance strategies and improved road safety.

Acknowledgments

This work was supported by the National Research Foundation of Korea (NRF) grant funded by the Korea government (MSIT) (No. 2022R1C1C1006507).

Declaration of interests

The authors declare no conflict of interest.

References

- Abdelmawla, A., Ma, S., Yang, J.J. and Kim, S.S. (2023), “Subsurface anomaly detection utilizing synthetic GPR images

- and deep learning model”, *Geomech. Eng.*, **33**(2), 203-209. <https://doi.org/10.12989/gae.2023.33.2.203>.
- Balasubramani, D.P. and Gopalakrishnan, V. (2020), “Subsurface object detection and characterizing using ground penetrating radar”, *Innov. Infrastruct. Solut.*, **5**, 101. <https://doi.org/10.1007/s41062-020-00352-5>.
- Basha, A.M. and Eldisouky, E.A. (2023), “Effect of eccentric loads on the behavior of circular footing with/without skirts resting on sand”, *Int. J. Geo-Eng.*, **14**, Article no. 13. <https://doi.org/10.1186/s40703-023-00192-z>.
- Dawood, T., Zhu, Z. and Zayed, T. (2020), “Deterioration mapping in subway infrastructure using sensory data of GPR”, *Tunn. Undergr. Sp. Tech.*, **103**, 103487. <https://doi.org/10.1016/j.tust.2020.103487>
- Gedney, S.D. (2011), “The perfectly matched layer (PML) absorbing medium. In Introduction to the Finite-Difference Time-Domain (FDTD) Method for Electromagnetics”, *Cham: Springer Int. Publishing*, 113-135. https://doi.org/10.1007/978-3-031-01712-4_6.
- Gidebo, F.A., Yasuhara, H. and Kinoshita, N. (2023), “Stabilization of expansive soil with agricultural waste additives: A review”, *Int. J. Geo-Eng.*, **14**, Article no. 14. <https://doi.org/10.1186/s40703-023-00194-x>.
- Guerrieri, M., Parla, G., Khanmohamadi, M. and Neduzha, L. (2024), “Asphalt pavement damage detection through deep learning technique and cost-effective equipment: A case study in urban roads crossed by tramway lines”, *Infrastruct.*, **9**(2), 34. <https://doi.org/10.3390/infrastructures9020034>.
- Huang, J., Yang, X., Zhou, F., Li, X., Zhou, B., Lu, S. and Slob, E. (2024), “A deep learning framework based on improved self-supervised learning for ground-penetrating radar tunnel lining inspection”, *Comput.-Aided Civil Infrastruct. Eng.*, **39**(6), 814-833. <https://doi.org/10.1111/mice.13042>.
- Irving, J. and Knight, R. (2006), “Numerical modeling of ground-penetrating radar in 2-D using MATLAB”, *Comput. Geosci.*, **32**(9), 1247-1258. <https://doi.org/10.1016/j.cageo.2005.11.006>.
- Jena, J., Mahed, G., Chabata, T., Doucoure, M. and Gibbon, T. (2024), “Monitoring and early warning detection of collapse and subsidence sinkholes using an optical fibre seismic”, *Cogent Eng.*, **11**, 2301152. <https://doi.org/10.1080/23311916.2023.2301152>.
- Kang, S., Yu, J.D., Han, W. and Lee, J.S. (2022), “Non-destructive detection of cavities beneath concrete plates using ground penetrating radar and microphone”, *NDT&E Int.*, **130**, 102663. <https://doi.org/10.1016/j.ndteint.2022.102663>.
- Kim, D., Kim, J. and Youn, H. (2024), “Automated ground penetrating radar B-scan detection enhanced by data augmentation techniques”, *Geomech. Eng.*, **38**, 29-44. <https://doi.org/10.12989/gae.2024.38.1.029>.
- Lai, W.W.L., Dérobert, X. and Annan, P. (2017), “A review of ground penetrating radar application in civil engineering: A 30-year journey from locating and testing to imaging and diagnosis”, *NDT&E Int.*, **96**, 58-78. <https://doi.org/10.1016/j.ndteint.2017.04.002>.
- Le, D.V. and Go, H. Y. (2024), “Development of a GPR simulation program to identify fouled layer in ballast railway ground”, Korean Geotechnical Society Spring National Conference 2024, March 21–22, Jeju, Korea.
- Li, F., Yang, F., Xie, Y., Qiao, X., Du, C., Li, C., Ru, Q., Zhang, F., Gu, X. and Yong, Z. (2024), “Research on 3D ground penetrating radar deep underground cavity identification algorithm in urban roads using multi-dimensional time-frequency features”, *NDT&E Int.*, **143**, 103060. <https://doi.org/10.1016/j.ndteint.2024.103060>.
- Liu, C., Du, Y., Yue, G., Li, Y., Wu, D. and Li, F. (2024), “Advances in automatic identification of road subsurface distress using ground penetrating radar: state of the art and future trends”, *Automat. Constr.*, **158**, 105185. <https://doi.org/10.1016/j.autcon.2023.105185>.
- Min, D.H. and Yoon, H.K. (2024), “Application of ground penetrating radar (GPR) coupled with convolutional neural network (CNN) for characterizing underground conditions”, *Geomech. Eng.*, **37**(5), 467-474. <https://doi.org/10.12989/gae.2024.37.5.467>.
- Min, K.S., Kim, D.M., Lee, D.Y., Jung, H.S. and Lee, Y.J. (2018), “Field and laboratory assessment of ground subsidence induced by underground cavity under the sewer pipe”, *Geomech. Eng.*, **16**(3), 285-293. <https://doi.org/10.12989/gae.2018.16.3.285>.
- Ministry of Land, Infrastructure and Transport, (2012), Road design manual.
- Sato, M. and Kuwano, R. (2015), “Influence of location of subsurface structures on development of underground cavities induced by internal erosion”, *Soils Found.*, **55**(4). <https://doi.org/10.1016/j.sandf.2015.06.014>.
- Shi, X. (2023), “More than smart pavements: Connected infrastructure paves the way for enhanced winter safety and mobility on highways”, *J. Infrastruct. Preserv. Resil.*, **1**(13). <https://doi.org/10.21203/rs.3.rs-31618/v1>.
- Shrestha, R. and Zhihou, Z. (2024), “Real time monitoring of urban roadway health: Utilizing GPR techniques for the early detection and classification of subsurface cavity diseases”, *Geosci.*, **2**, Article no. 74. <https://doi.org/10.1007/s44288-024-00069-3>.
- Tong, Z., Gao, J. and Yua, D. (2020), “Advances of deep learning applications in ground-penetrating radar: A survey”, *Constr. Build. Mater.*, **258**, 120371. <https://doi.org/10.1016/j.conbuildmat.2020.120371>.
- Wang, Z., Zhu, J. and Ma, T. (2024), “Monitoring of pavement subgrade settlement: influencing factor, measurement, and advancement”, *Measurement*, **237**, 115225. <https://doi.org/10.1016/j.measurement.2024.115225>.
- Warren, C., Giannopoulos, A. and Giannakis, I. (2016), “gprMax: Open source software to simulate electromagnetic wave propagation for ground-penetrating radar”, *Comput. Phys. Commun.*, **209**, 163-170. <https://doi.org/10.1016/j.cpc.2016.08.020>.
- Yamaguchi, T., Mizutani, T., Meguro, K. and Hirano, T. (2022), “Detecting subsurface voids from GPR images by 3-D convolutional neural network using 2-D finite difference time domain method”, *IEEE J. Sel. Top. Appl. Earth Obs. Remote Sens.*, **15**, 3061-3073. <https://doi.org/10.1109/JSTARS.2022.3165660>.
- Zhang, F., Liu, B., Liu, L., Wang, J., Lin, C., Yang, L., Li, Y., Zhang, Q. and Yang, W. (2019), “Application of ground penetrating radar to detect tunnel lining defects based on improved full waveform inversion and reverse time migration”, *Near Surface Geophys.*, **17**(2), 127-139. <https://doi.org/10.1002/nsg.12032>
- Zhang, W., Xin, G., Long, G. and Song, L. (2023), “Ground penetrating radar forward modelling of roads based on random media model”, *Acta Geod. Geophys.*, **58**, 109-122. <https://doi.org/10.1007/s40328-023-00403-0>.